Received: 23 December 2021 | Revised: 3 May 2022 | Accepted: 13 May 2022

DOI: 10.1002/mp.15773

TECHNICAL NOTE

MEDICAL PHYSICS

# Technical note: Evaluation of methods for reducing edge current density under electrode arrays for tumor-treating fields therapy

**Heehun Sung**[1] | **Yunhui Jo**[2] | **Geon Oh**[1] | **Yongha Gi**[1] | **Hyunwoo Kim**[1,3] | **Sangmin Park**[1,3] | **Jaehyeon Seo**[1] | **Myonggeun Yoon**[1,3]

[1]Department of Bioengineering, Korea University, Seoul, Republic of Korea

[2]Institute of Global Health Technology (IGHT), Korea University, Seoul, Republic of Korea

[3]FieldCure Ltd, Seoul, Republic of Korea

**Correspondence**
Myonggeun Yoon, Department of Bioengineering, Korea University, Anam-ro 145, Seongbuk-Gu, Seoul 02842, Republic of Korea.
Email: radioyoon@korea.ac.kr

**Funding information**
National Research Foundation of Korea (NRF), Grant/Award Number: 2021R1A2C2008695

## Abstract

**Background:** Tumor-treating fields (TTFields) therapy is increasingly utilized clinically because of its demonstrated efficacy in cancer treatment. However, the risk of skin burns must still be reduced to improve patient safety and posttreatment quality of life.

**Purpose:** The purpose of this study was to evaluate the methods of constructing electrode arrays that reduce current density exceeding threshold values, which can cause skin burns during TTFields therapy.

**Methods:** Electrode and body models were generated using COMSOL software. The body model had the dielectric properties of the scalp. The average current density beneath the central region of the electrode was maintained at ~31 mA/cm$^2$ RMS. The deviations in current density at the edges of the electrode were reduced by three methods: adjustment of the ceramic thickness ratio of the center to the edge from 1/5 to 4/5, adjustment of the radius of the metal plate from 5.0 to 8.0 mm, and insertion of an insulator of width 0.5 to 2 mm at the edge.

**Results:** While using a single circular electrode, adjustment of the ceramic thickness ratio, adjustment of the metal plate radius, and insertion of an insulator near the edge reduced the deviations of current density by 14.6%, 67.7%, and 75.3%, respectively. Similarly, while using circular electrode arrays, inserting an insulator at the edge of each electrode reduced the deviations of current density significantly, from 8.62 to 2.40 mA/cm$^2$.

**Conclusions:** Insertion of an insulator at the edge of each electrode was found to be the most effective method of attaining uniform current density distribution beneath the electrode, thereby lowering the risk of adverse effects of TTFields therapy.

**KEYWORDS**
current density, edge current, electrode arrays, tumor-treating fields

## 1 | INTRODUCTION

Tumor-treating fields (TTFields) therapy is the delivery of a low-intensity electric field (1–3 V/cm) at intermediate frequency (100–300 kHz) to dividing cells, thereby inhibiting cell division.[1] Because TTFields have a greater effect on dividing cells than on nondividing cells, it has a greater effect on cancer cells, which divide more frequently, than on normal cells, which divide relatively infrequently.[2] The inhibitory effect of TTFields on cell division increases in proportion to the intensity of the electric field and the duration of its application. A recent clinical trial also showed that higher electric field intensity was associated with a higher patient survival rate.[1,3] The rates of hematological, infectious, and gastrointestinal side effects were shown to be lower, and quality of life better with TTFields therapy than with chemotherapy.[4] The addition of TTFields therapy to chemotherapy has shown better therapeutic outcomes than chemotherapy alone in patients with glioblastoma

  

multiforme (GBM).[5,6] For example, the treatment of GBM patients with chemotherapy plus TTFields therapy resulted in longer median progression-free survival (7.2 vs. 4.0 months), median overall survival (20.5 vs. 15.8 months), and higher 2-year survival rates (43% vs. 29%) than chemotherapy alone.[5,6]

TTFields therapy is currently performed by attaching electrodes onto the skin to deliver an electric field.[7] In general, the current generated by the electric field produces heat, increasing the risk of burns on the skin when the electric field intensity is over the tolerance limit.[8] The threshold of current density recommended to prevent skin burns has been reported to be 100 mA/cm$^2$ RMS, whereas the maximum current density applied during TTFields therapy is limited to 31 mA/cm$^2$ RMS or ~1/3 of the threshold current density.[2] Despite this relatively safe upper limit of current density, however, skin burns may occur in patients receiving TTFields therapy.[5,6,8,9]

One drawback to the electrodes currently used for TTFields therapy is that the distribution of the electric field beneath the electrode is not uniform, with a high electric field at the edges of the electrodes.[10] According to Ohm's law, which states that electric field and current density are linearly related, the current density distribution at the contact surfaces of the electrodes is also not uniform,[11] with the intensity of current density increasing from the center to the edges.[12] Thus, even when the average current density is 31 mA/cm$^2$ RMS, its nonuniform distribution results in a higher current density near the edges, increasing the risk of skin burns near the edges. Although current density at the edges can be reduced by reducing the average current density to below 31 mA/cm$^2$ RMS, this would result in an overall reduction in electric field intensity, diminishing the therapeutic effects of TTFields therapy. Thus, to maximize this therapeutic effect, it is necessary to develop a method that allows the uniform distribution of current density on the skin by reducing the current density near the edges of the electrode while maintaining threshold current density. The present study therefore devised and evaluated methods of constructing electrodes that provide uniform current density distribution while reducing current density at the edges that exceed the threshold value for TTFields therapy.

## 2 | MATERIALS AND METHODS

This study utilized the finite element method to evaluate the current density distribution of electrodes for TTFields therapy. A body model, to which the electrode was attached, had the shape of a rectangular cuboid, with a height and width of 10 cm each and a thickness of 5 cm. The body model had the dielectric properties of the scalp, including a conductivity of 0.25 S/m and a relative permittivity of 5000.[13] Each electrode was modeled to closely represent Optune systems, which are used in clinical practice.[5,6,8] Each electrode was composed of a metal plate (conductor), a ceramic, and a hydrogel, with thicknesses of 0.1, 1.0, and 2.0 mm, respectively; conductivities of 6E + 7, 1E − 13, and 0.1 S/m, respectively; and relative permittivities of 1, 5000, and 100, respectively (Table 1).[2,13,14] Each circular electrode was 18 mm in diameter, whereas each square electrode was 18-mm wide (Figure 1). Each electrode array consisted of 3 × 3 electrodes separated by 22 and 33 mm along with two perpendicular directions, similar to arrays used in clinical practice.[13,15,16]

**TABLE 1** Properties of materials

| Material | Conductivity [S/m] | Relative permittivity |
|---|---|---|
| Body | 0.25 | 5000 |
| Conductor (plate) | $6.0 \times 10^{7}$ | 1.00 |
| Ceramic | $1.0 \times 10^{-13}$ | 5000 |
| Hydrogel | 0.10 | 100 |
| Insulator (polyethylene) | $1.0 \times 10^{-6}$ | 2.25 |

The mesh utilized had a maximum element size of 0.55 cm, a minimum element size of 0.04 cm, a maximum element growth rate of 1.4, a curvature factor of 0.4, and a resolution of narrow regions of 0.7. Both the body and electrode models were generated using COMSOL Multiphysics, version 5.5 (COMSOL Inc., Sweden). The ability to reduce higher current density at electrode edges was tested by varying three aspects of the system: (1) adjusting the thickness ratio of the ceramic, (2) adjusting the radius of the metal plate, and (3) inserting an insulator made of polyethylene into the electrode.

The current density distribution beneath the electrode was tested by delivering an electric field of 200 kHz to the electrode attached to the body model, while maintaining the average current density at the central region (radius ≤4.5 mm) of the electrode at ~31 mA/cm$^2$ RMS. Simulations were performed using the COMSOL electric currents interface. The uniformity of the current density distribution was evaluated by calculating the deviation of current density from 31 mA/cm$^2$ RMS, which was defined as the threshold current density to avoid skin burns.

## 3 | RESULTS

### 3.1 | Reference electrode model: single circular and square electrode

Schematics of the circular and square electrode models are displayed in Figures 2a,d, respectively. Measurements of the distributions of current density showed that current density exceeded 50 mA/cm$^2$ RMS at the edges of both the circular and square electrodes (Figure 2b,e, red regions). Profiles of current density under the cir-

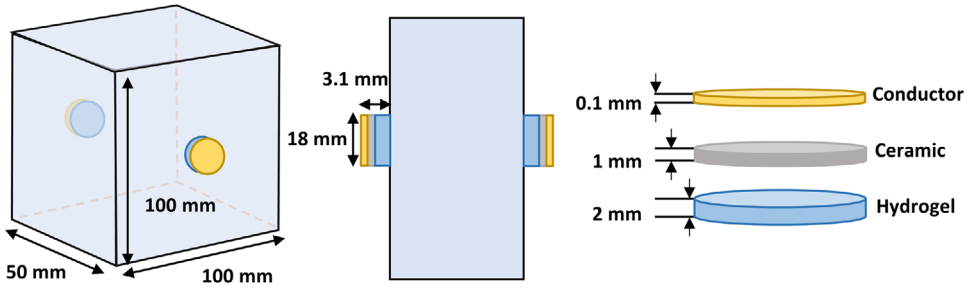


**FIGURE 1** Geometry of the body model and circular electrode model. Each electrode consisted of a conductor plate, a ceramic insulator, and a hydrogel.

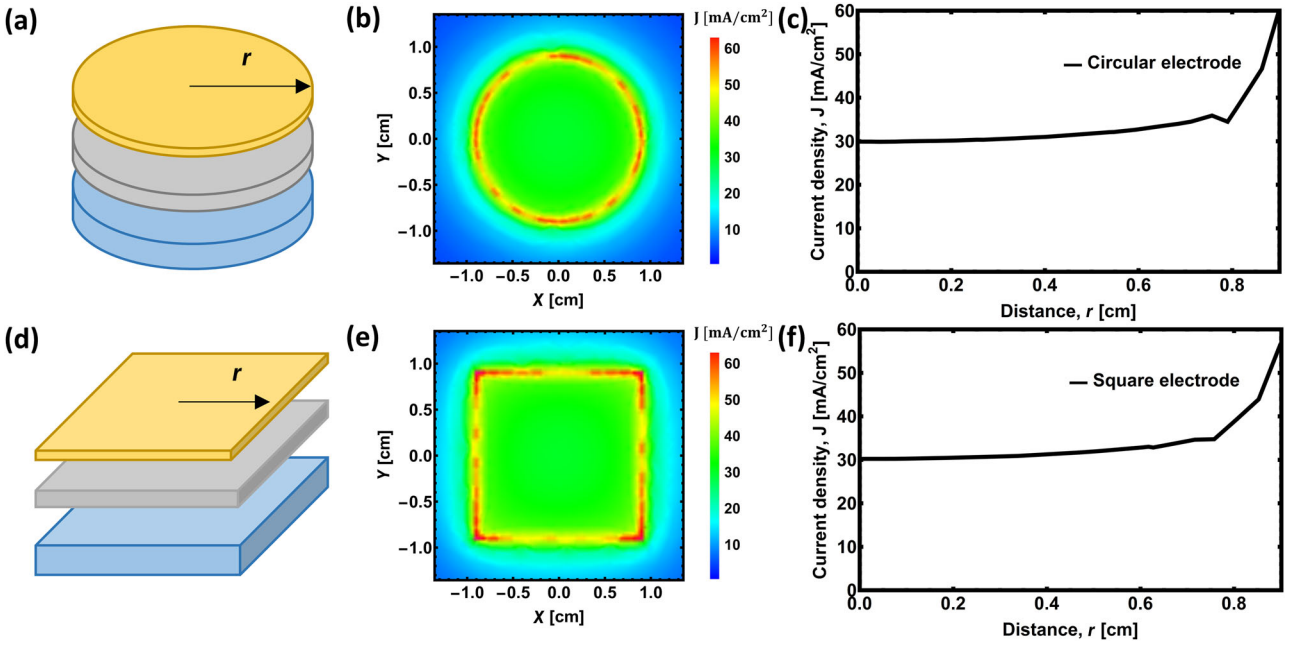


**FIGURE 2** Distribution of current density in a single electrode. (a) Circular electrode model. (b) Distribution of current density under the circular electrode. (c) Profile of current density under the circular electrode along the *r*-axis. (d) Square electrode model. (e) Distribution of current density under the square electrode. (f) Profile of current density under the square electrode along the *r*-axis.

cular and square electrodes along the *r*-axis suggested that current density increased as the distance along the *r*-axis increased (Figure 2c,f). Although the threshold current density in the central region of the electrode was set at ~31 mA/cm$^2$ RMS, the current density at the edges was significantly higher, indicating a high risk of skin burns in this region. The analysis of current density distribution showed that the deviations of current density for circular and square electrodes were 7.96 and 8.47 mA/cm$^2$, respectively.

## 3.2 | Adjustment of the thickness ratio of the ceramic of circular electrodes

Figure 3a shows a side view of a circular electrode model with variable thickness ratios ($h_r$), defined as the ratio of thickness at the center to a basic thickness ($h_0$) of 2 mm. To evaluate the effect of the ratio of the thickness of the center to the edge of the ceramic, a ceramic with a basic thickness of 2.0 mm was cut radially along the direction of the electrode center (Figure 3a). Profiles of current density for various thickness ratios showed that the current density at the edge of the electrode decreased as the thickness ratio decreased, with a maximum effect observed when the adjustment of the thickness ratio was 1/5 (Figure 3b). Analysis of current density distribution for the adjustment of the thickness ratio of 1/5 showed that the deviations of current density decreased from 7.96 to 6.80 mA/cm$^2$, a reduction of 14.6% (Figure 3c,d). These findings suggested that, although adjusting the thickness ratio of the ceramic can reduce the deviation of current density beneath the electrode, the effect was not significant, with a maximum 14.6% reduction in the deviation of current density.

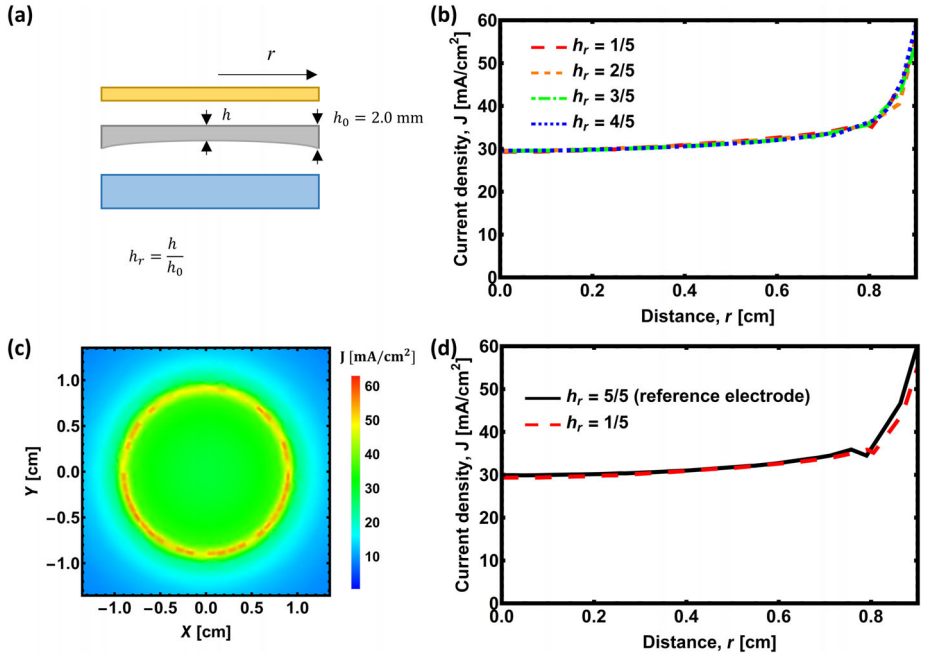


**FIGURE 3** (a) Model of a circular electrode with variable thickness ratios of the ceramic. (b) Profiles of current density along the *r*-axis as a function of the thickness ratio of the ceramic. (c) Distribution of current density for electrodes with a thickness $h_r$ of 1/5. (d) Profiles of current density along the *r*-axis for electrodes of thicknesses $h_r$ of 1/5 and 5/5.

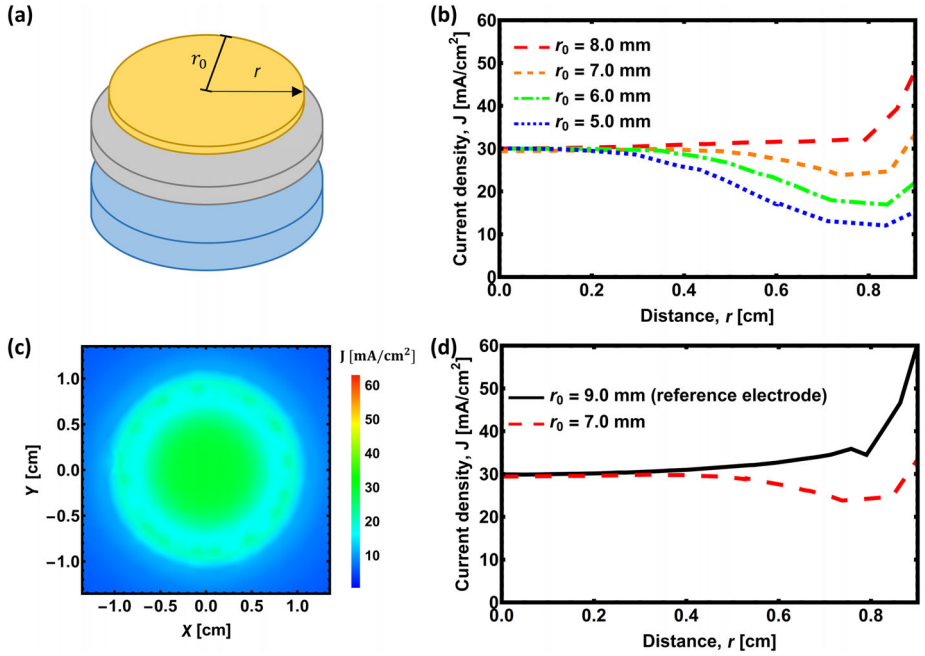


**FIGURE 4** (a) Model of a circular electrode with variable radii of the conductor plate, with $r_0$ defined as the radius of the metal plate. (b) Profiles of current density along the *r*-axis as a function of the radius of the plate. (c) Distribution of current density with an $r_0$ of 7.0 mm. (d) Profiles of current density along the *r*-axis for radii of 7.0 and 9.0 mm.

## 3.3 | Adjustment of the radius of a metal plate for circular electrodes

Figure 4a shows a schematic of a circular electrode model with a variable radius. The radius of the conductor plate ($r_0$) was set at 9 mm for the reference electrode (Figure 2a). To evaluate the effects of adjusting the radius of the conductor plate, $r_0$ was changed from 8 to 5 mm. Profiles of current density for various $r_0$ showed that the current density near the edge of the electrode

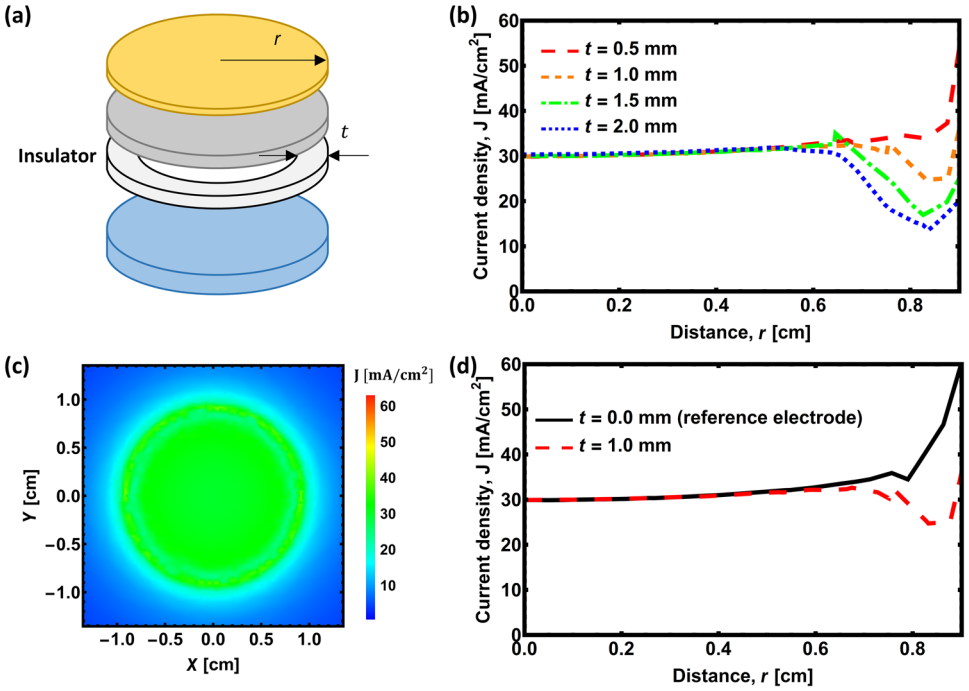


**FIGURE 5** (a) Model of a circular electrode with an inserted insulator. (b) Profiles of current density along the *r*-axis as a function of the width of the insulator ring. (c) Distribution of current density for *t* of 1.0 mm. (d) Profiles of current density along the *r*-axis for *t* of 1.0 and 0.0 mm.

decreased as $r_0$ decreased, with an $r_0$ of 5 mm having the maximum effect (Figure 4b). At an $r_0$ of 5 mm, however, the current density at the edge was reduced too much, resulting in a nonuniform distribution of current density underneath the electrode. The uniformity of current density was optimal when $r_0$ was 7 mm, at which the deviation of current density decreased from 7.96 to 2.57 mA/cm$^2$, a reduction of 67.7% (Figure 4c,d). These results suggest that adjusting the radius of the conductor plate can effectively reduce the deviation of current density beneath the electrode, with a maximum 67.7% reduction in the deviation of current density.

## 3.4 | Insertion of an insulator near the edge of a circular electrode

Figure 5a shows a schematic of a circular electrode model with an inserted insulator ring, with *t* defined as the width of the insulator ring. To evaluate the effect of inserting an insulator ring near the edge of the electrode, *t* was changed from 0.5 to 2.0 mm. Profiles of current density for various *t* values showed that the current density near the edge of the electrode decreased as *t* increased, with a *t* of 2.0 mm having the maximum effect (Figure 5b). At this width, however, the current density near the edge region was reduced too much, resulting in the nonuniform distribution of current density underneath the electrode. The uniformity of current density was optimal when *t* was 1.0 mm, at which the deviation of current density decreased from 7.96 to 1.97 mA/cm$^2$, a reduction of 75.3% (Figure 5c,d). These results suggest that inserting an insulator near the edge of the electrode can effectively reduce the deviation of current density beneath the electrode, with a maximum 75.3% reduction in the deviation of current density.

## 3.5 | Insertion of an insulator near the edge of a square electrode

Figure 6a shows a schematic of a square electrode model with an inserted insulator. Profiles of current density for various *t* showed that the current density near the edge region of the electrode decreased as *t* increased, with a maximum effect for a *t* of 2.0 mm (Figure 6b). Similar to the circular electrode model (Figure 5b), the current density at the edges of the square electrode was reduced too much when *t* was 2.0 mm, resulting in a nonuniform distribution of current density beneath the electrode. The uniformity of current density was optimal when *t* was 1.0 mm, at which the deviation of current density decreased from 8.47 to 2.47 mA/cm$^2$, a reduction of 70.8% (Figure 6c,d). These results suggest that inserting an insulator near the edge of the electrode can effectively reduce the deviation of current density beneath the electrode, regardless of electrode shape.

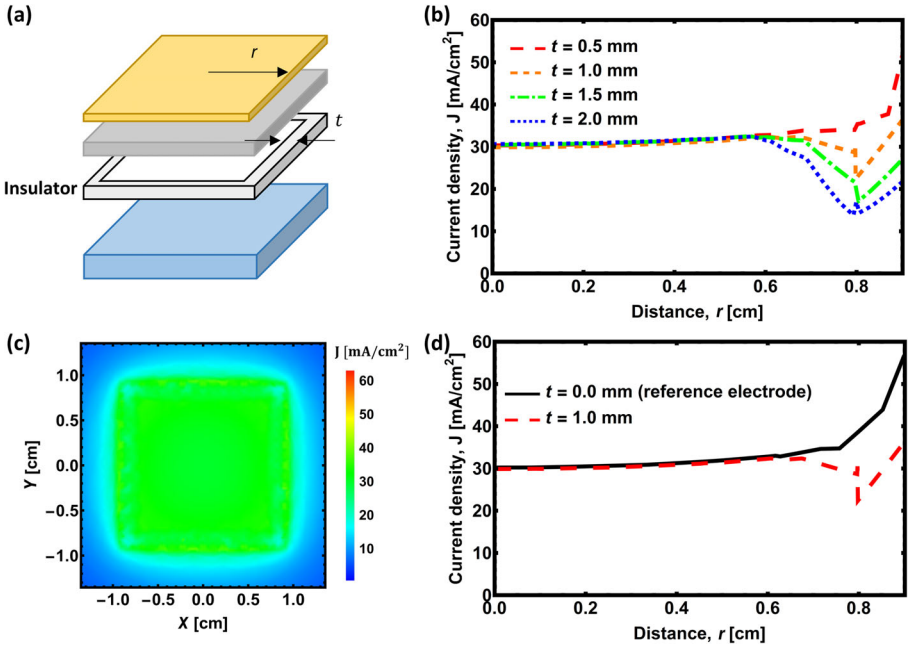


**FIGURE 6** (a) Schematic of a model of a square electrode with an inserted insulator. (b) Profiles of current density along the *r*-axis as a function of the width of the insulator. (c) Distribution of current density for *t* of 1.0 mm. (d) Profiles of current density along the *r*-axis for *t* of 1.0 and 0.0 mm.

### 3.6 | Insertion of an insulator near the edge of a circular electrode array

Figure 7a shows a schematic of a model of a circular electrode array, consisting of 3 × 3 electrodes and similar to arrays currently being used in clinical practice.[13] Similar to findings with single electrodes, the current density profile under the electrode array along the *r*-axis also showed that the current density increases near the edge region of each electrode (Figure 7b, "A,", "B,", and "C"). Analysis showed that the average deviation of current density for a circular electrode array was 8.62 mA/cm$^2$ (Figure 7c). To evaluate the effect of the insertion of an insulator ring at the edge of the electrode, an insulator ring with a *t* of 1.0 mm was inserted under the ceramic (Figure 7d), reducing the current density near the edge region of the electrode (Figure 7e). Insertion of the insulator ring increased the uniformity of current density and decreased the deviation of current density from 8.62 to 2.40 mA/cm$^2$, a 72.2% reduction (Figure 7f). These results suggest that inserting an insulator near the edge of an electrode can effectively reduce the deviation of current density beneath the electrode array, with a maximum 72.2% reduction in the deviation of current density.

## 4 | DISCUSSION

The simulation results obtained in the present study showed that the deviations of current density for a single circular electrode were reduced by 14.6% by adjusting the ceramic thickness ratio, 67.7% by adjusting the metal plate radius, and 75.3% by inserting an insulator near the edge, indicating that the latter was the most effective method of attaining a uniform current density distribution beneath the electrode. Inserting an insulator at the edge of each electrode in an array of circular electrodes also increased the uniformity of current density by reducing the deviations of current density from 8.62 to 2.40 mA/cm$^2$.

This study evaluated three methods of reducing current density to ensure that it does not exceed the threshold value in TTFields therapy. A gradual reduction in the thickness of the electrode ceramic from the edges to the center resulted in a relatively uniform current density distribution by creating a difference in resistance between the center and edge regions. However, compared with the other two methods, this method was not sufficiently effective in reducing current density exceeding the threshold at the edge region. The second method, involving adjustment of the radius of the metal plate in the electrode, prevents an increase in current density at the edges by spreading the current. Compared with the other two methods, this method was relatively effective in reducing current density at the edges. However, this electrode model may be unstable due to structural vulnerability, as the base plate was smaller than the upper structure, that is, the ceramic. The third method, involving the insertion of insulating material near the edge of the electrode, increases resistance at the edges of the electrode, while reducing the flow of current to the edges. Of the three methods tested, the

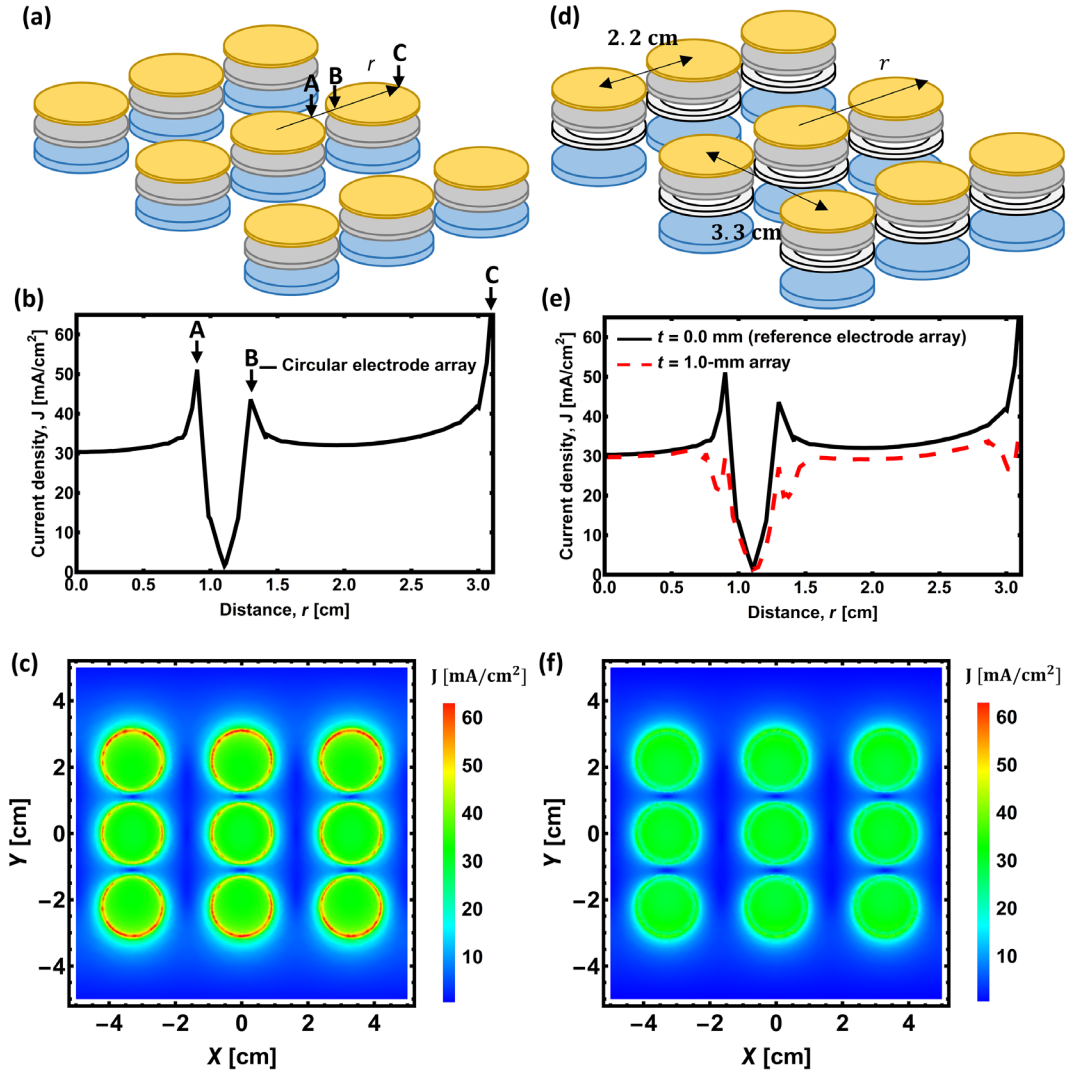


**FIGURE 7** (a) Model of a circular electrode array. (b) Profile of current density along the *r*-axis for a circular electrode array. (c) Distribution of current density for a circular electrode array. (d) Model of a circular electrode with an inserted insulator ring. (e) Profiles of current density along the *r*-axis in a circular electrode array with inserted insulator ring having *t* values of 1.0 and 0 mm. (f) Distribution of current density in a circular electrode array with an inserted insulator ring having a *t* of 1.0 mm.

latter was the most effective at attaining uniform current density distribution with a stable structural model.

In practice, patient tissues differ in conductivity and permittivity. For example, the conductivity of scalp tissue ranges from 0.14 to 0.45 S/m and its relative permittivity ranges from 1000 to 10 000. To investigate whether these differences among individuals can alter results, the distributions of current density were assessed for the minimum and maximum values of scalp tissue (i.e., body model). Insertion of insulator rings with a width (*t*) of 1.0 mm into circular electrode arrays resulted in deviations of current density distributions of 3.60 and 2.85 mA/cm$^2$ for the minimum and maximum values of scalp tissue, respectively. Although the reduction rates in the deviations of current density distributions depended on the values chosen, there were no substantial differences among them. The minimum and maximum values chosen for scalp tissue resulted in reductions of 58.2% and 66.9%, respectively, in deviations of current density distributions. These results suggest that, although the rates of reduction in deviations of current density distributions are dependent on tissue properties, the suggested method can be effective in providing uniform current density distribution beneath the electrode.

In general, the current density distribution beneath each electrode depends on its location in the electrode array. Current density distributions differ slightly among electrodes in an electrode array. Although the current density beneath the center electrode is relatively symmetric, the current density distributions beneath the other eight electrodes are not symmetric. Therefore, to

attain a uniform current density distribution more effectively, this nonuniform current distribution in an electrode array should also be considered.

## 5 | CONCLUSIONS

This study investigated the methods of reducing increases in current density at the edges of electrodes. Both the insertion of an insulator at the edge of each electrode and the adjustment of the radius of the metal plate were found to be effective in attaining uniform current density distribution beneath the electrode. In contrast, controlling the thickness ratio of the ceramic was less effective in providing a uniform current density distribution. Results using an electrode array suggested that insertion of an insulator at the edge of each electrode resulted in a uniform current density distribution, thereby reducing the risk of skin burns in patients undergoing TTFields therapy.

## ACKNOWLEDGMENTS

This work was supported by a grant from the National Research Foundation of Korea (NRF), funded by the Korean government (MSIT) (2021R1A2C2008695).

## CONFLICT OF INTEREST

The authors declare that there is no conflict of interest that could be perceived as prejudicing the impartiality of the research reported.

## REFERENCES

1. Kirson ED, Gurvich Z, Schneiderman R, et al. Disruption of cancer cell replication by alternating electric fields. *Cancer Res*. 2004;64(9):3288-3295.
2. Kirson ED, Dbalý V, Tovaryš F, et al. Alternating electric fields arrest cell proliferation in animal tumor models and human brain tumors. *Proc Natl Acad Sci USA*. 2007;104(24):10152-10157.
3. Ballo MT, Urman N, Lavy-Shahaf G, Grewal J, Ze Bomzon, Toms S. Correlation of tumor treating fields dosimetry to survival outcomes in newly diagnosed glioblastoma: a large-scale numerical simulation-based analysis of data from the phase 3 EF-14 randomized trial. *Int J Radiat Oncol Biol Phys*. 2019;104(5):1106-1113.
4. Davies AM, Weinberg U, Palti Y. Tumor treating fields: a new frontier in cancer therapy. *Ann NY Acad Sci*. 2013;1291(1):86-95.
5. Stupp R, Taillibert S, Kanner AA, et al. Maintenance therapy with tumor-treating fields plus temozolomide vs temozolomide alone for glioblastoma: a randomized clinical trial. *JAMA*. 2015;314(23):2535-2543.
6. Stupp R, Taillibert S, Kanner A, et al. Effect of tumor-treating fields plus maintenance temozolomide vs maintenance temozolomide alone on survival in patients with glioblastoma: a randomized clinical trial. *JAMA*. 2017;318(23):2306-2316.
7. Murphy J, Bowers ME, Barron L. Optune®: practical nursing applications. *CJON*. 2016;20(5):S14-S19.
8. Stupp R, Wong ET, Kanner AA, et al. NovoTTF-100A versus physician's choice chemotherapy in recurrent glioblastoma: a randomised phase III trial of a novel treatment modality. *Eur J Cancer*. 2012;48(14):2192-2202.
9. Pless M, Weinberg U. Tumor treating fields: concept, evidence and future. *Expert Opin Investig Drugs*. 2011;20(8):1099-1106.
10. Korshoej AR, Hansen FL, Mikic N, von Oettingen G, Sørensen JCH, Thielscher A. Importance of electrode position for the distribution of tumor treating fields (TTFields) in a human brain. Identification of effective layouts through systematic analysis of array positions for multiple tumor locations. *PLoS One*. 2018;13(8):e0201957.
11. Griffiths DJ. Introduction to electrodynamics. *Am J Phys*. 2005;73:574.
12. Newman J. Resistance for flow of current to a disk. *J Electrochem Soc*. 1966;113(5):501-502.
13. Wenger C, Salvador R, Basser PJ, Miranda PC. The electric field distribution in the brain during TTFields therapy and its dependence on tissue dielectric properties and anatomy: a computational study. *Phys Med Biol*. 2015;60(18):7339.
14. Young HD, Freedman RA, Ford AL. University physics with modern physics 13th edition. *Haettu*. 2012;11:2020.
15. Bomzon Z, Urman N, Wenger C, et al. Modelling tumor treating fields for the treatment of lung-based tumors. Paper presented at: 2015 37th Annual International Conference of the IEEE Engineering in Medicine and Biology Society (EMBC). 2015.
16. Miranda PC, Lomarev M, Hallett M. Modeling the current distribution during transcranial direct current stimulation. *Clin Neurophysiol*. 2006;117(7):1623-1629.

**How to cite this article:** Sung H, Jo Y, Oh G, et al. Technical note: Evaluation of methods for reducing edge current density under electrode arrays for tumor-treating fields therapy. *Med. Phys*. 2022;49:4837-4844.
https://doi.org/10.1002/mp.15773